STRUCTURAL AND OPTICAL CHARACTERIZATION OF PMMA SURFACE TREATED IN LOW POWER NITROGEN AND OXYGEN RF PLASMAS

D. DORRANIAN*, Z. ABEDINI[a], A. HOJABRI[a], M. GHORANNEVISS
Plasma Physics Research Center, Science and Research Campus,
Islamic Azad University, Tehran, Iran
[a]*Physics Department, Science Faculty, Islamic Azad University-Karaj Branch, Karaj, Iran.*
**E-mail: doran@srbiau.ac.ir*

Oxygen and nitrogen plasmas are used to modify the Poly methyl methacrylate (PMMA) polymer surface and results are compared. Samples are treated in a plane parallel capacitively coupled RF discharge at 13.56 MHz frequency and 25 W power for different times. The modified surfaces are characterized by Fourier transform infrared spectrometer (ATR-FTIR) and atomic force microscopic (AFM) micrographs. By the results of contact angle measurement, polar and disperse parts of surface energy are observed. Real and imaginary parts of refractive index and dielectric constant for different samples are calculated using the transmission and reflection spectrum of samples and the energy gaps are calculated. RMS roughness of samples surface is found to be changed more effectively by nitrogen plasma compare to oxygen plasma but the molecular structure of the treated surfaces is noticeably affected by oxygen plasma. The contribution of the polar part of surface energy is decreased with treatment time. The water contact angle is decreased noticeably by this treatment while the energy gap of samples is not changed.

(Received September 2, 2009; accepted September 29, 2009)

Keywords: Surface modification, Optical properties, Hydrophilic, Surface energy

1. Introduction

Traditionally, polymer matrix composites have been thought as insulating materials and have been used in applications like power tool handles, cable, jackets, capacitor films and electronic packaging materials [1]. Especially the electrical and optical properties of polymers have been extensively investigated due to their applications in optical devices recently. Polymeric materials have unique properties such as low density, light weight, and high flexibility and are widely used in various industrial sectors [2]. In recent years the great progress in understanding polymer surface phenomena and development in their theoretical description have been done. Forces occurring on polymer surfaces depend on interactions between macromolecules, which are different inside of material and on the phase boundary. Several reactions occur at the polymer surface during modification such as oxidation, crosslinking, degradation and isomerisation (rotation of functional groups) [3]. The determination of the optical constants of polymers such as refractive index and extinction coefficient is also important for optical applications. Furthermore, the refractive index and optical band gap are the fundamental parameters of an optical material, because these are closely related to the electronic properties of the material [4].

Poly methyl-methacrylate (PMMA) as a polymer waveguide has attracted much attention for use as optical components and in optoelectronic devices due to its low cost and volume productivity. PMMA is an important and interesting polymer because of attractive physical and optical properties decisive about its broad application. This is the thermoplastic material with the good tensile strength and hardness, high rigidity, transparency, good insulation properties and thermal stability dependent on tactility. PMMA have some disadvantages such as brittleness and low chemical resistance which can be eliminated by chemical or physical modification. PMMA contains both hydrophobic (methylene) and hydrophilic (carbonyl) groups in each unit [3]. In addition, it is found that it can produce a large refractive index difference with acryl amide-based photopolymer [5].

Most polymeric surfaces as well as PMMA are inert, hydrophobic in nature and usually have a low surface energy, whereas hydrophilicity is needed for reaching a good adhesion to other substances. Therefore, they do not possess specific surface properties needed in various applications, and their surfaces need to be treated to obtain polymers with desired surface properties in various instances [3,6,7]. The possibility of selective modification of the surface, while keeping bulk characteristics unchanged, has greatly increased the applicability of polymers [2,8,9]. For instance, the adhesion of metal films to polymer, a subject of great concern in food packaging, flexible cables, and connectors in microelectronics, is significantly improved as the free surface energy is enhanced. Moreover, actived polymers have been used as base for tissue integration, cell seeding, and bacterial growth [8].

Physical surface modification methods range from simple flame and corona treatments to more complicated and advanced techniques such as UV, gamma-ray, electron beam irradiations, ion beam, plasma, and laser treatments [2,3,6-10]. These treatments lead the breakage of covalent bonds, promotion of cross linkages, formation of carbon clusters, liberation of volatile species and in certain cases creation of new chemical bonds [11].

Between them plasma treatments are used to improve wettability, printability, sealability, and adhesion properties of polymers as well as to enhance polymer resistance to mechanical failure. These treatments are also employed to deposit thin polymer films on polymer surfaces or other packaging materials such as metals and glass [6]. Plasma processes have distinct advantages, and these benefits make plasma treatments an ideal means of modifying polymer surface characteristics. Modifications are limited to the surface layer to a depth of typically 0.005 to 0.05 μm, which leaves the bulk properties of the polymer unaffected. The intensity of plasma treatments at the surface is stronger than that of more penetrating surface modification methods, thus providing fast treatment of the surface with a layer of highly enriched functional species. The modified layer formed is fairly uniform in thickness over the whole surface and long lived. Heat sensitive polymeric materials can be successfully treated by plasmas. Three dimensional objects can be treated without any difficulty by plasma processes and plasma surface treatments are friendly to the environment [6,12].

In this work, nitrogen and oxygen RF plasmas are employed for the treatment of PMMA sheets and results are compared.

This paper is organized as follow. After introduction in Sec. 1, experimental details are presented in Sec. 2. Sec. 3 is devoted to results and discussion, and conclusion is in Sec. 4.

2. Experimental

In this experiment PMMA sheets (thickness 1.88 mm) are treated in plane parallel capacitively coupled RF discharge in oxygen and nitrogen plasmas. The PMMA molecular structure is shown in Fig. 1. Because of different analysis samples are cut in 1×1 cm, 1×5 cm and 2×4 cm pieces (as required for analysis machines) and cleaned in alcohol ultrasonically.

Radio frequency glow discharge plasma is generated using KX1050 plasma generator from EMITECH CO. at 13.56 Hz frequency and 25 W power. The exposure time is varied from 120 to 600 s. Samples are laid on a flat electrode connected to RF generator perpendicular to the direction of electric field. Base pressure of plasma reactor is 0.001 Torr which is increased to 0.5 Torr after gas feeding.

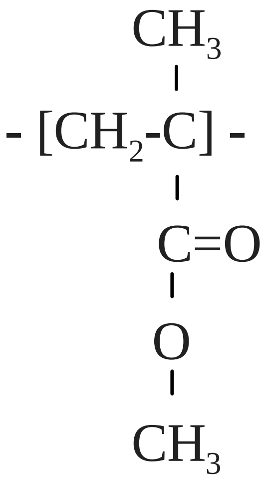

$$-[CH_2-C(CH_3)(C(=O)-O-CH_3)]-$$

Fig. 1. Chemical structure of Poly methyl-methacrylate (PMMA).

To characterize the structure of modified samples, attenuated total reflectance Fourier transform infrared (ATR-FTIR) analysis is performed using a FT-IR instrument (BRUKER). PMMA surface morphology is observed using Auto Probe CP atomic force microscope (AFM: Park Scientific Instrument). Static contact angles with water and diodo-methane are measured using the sessile drop method with contact angle measurement equipment (Kruss G10). All contact angles are the mean value of four measurements on different parts of the sheets. Surface tension, polar and disperse parts of the surface tension are obtained by Owens – Wendt and Wu methods. Varian Cary-500 spectrophotometer is used for recording UV-Vis-NIR transmission and reflection spectrum of the pristine and treated PMMA samples. The weight loss induced by degradation is estimated by weighting the sample before and after plasma treatment.

3. Results

3.1. Surface structure and morphology

The most important characteristics of the surface of samples are determined by the functional groups present in the surface layer. Fourier transform infrared (ATR-FTIR) spectroscopy is used for this purpose. FTIR spectrums of pristine and treated samples are shown in Figs. 2 and 3. Fig. 2 (a) and (b) belong to oxygen plasma treated samples. In Fig. 2 (a) results for 2, 4 and 6 minutes treated samples are presented and in Fig. 2 (b) results for 8 and 10 minutes treated samples are shown all beside the spectrum of pristine sample. As can be seen in Fig. 2 (a) immersion of PMMA in oxygen plasma for less than 6 minutes decreases the transmission of samples to about 80% of pristine sample in the range of 700 to 4000 cm^{-1} of electromagnetic radiation. However compare to the spectrum of the pristine sample there is a smaller peak magnitude in C-H stretching bonds at about 3000 cm^{-1}, but the intensity of peaks at 1130 cm^{-1} and 1600 cm^{-1} correspond to C-O and C=O groups increase. These changes increase with time up to 6 minutes treatment. After 6 minutes everything seems to be changed back. Noticeable difference between the transmission spectrum of pristine sample and the samples which are treated in oxygen plasma for 8 and 10 minutes is in the range of 2600 to 3700 cm^{-1}. This region mainly belongs to O-H vibration group and C-H stretch group. According to FTIR spectrum the intensity of the peaks belong to these groups decrease when the treatment time in oxygen plasma exceeds 6 minutes.

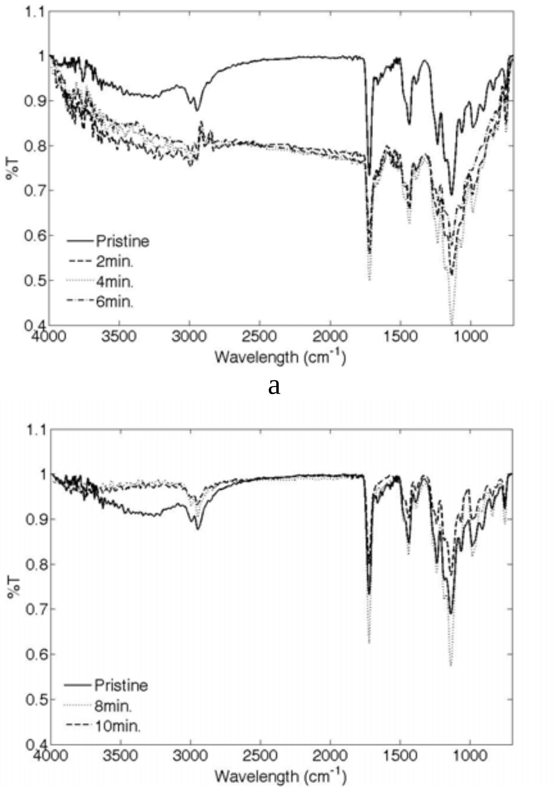

a

b

Fig. 2. ATR-FTIR spectrum for pristine sample beside treated samples for 2, 4 and 6 minutes (a) and 8 and 10 minutes (b) in oxygen plasma.

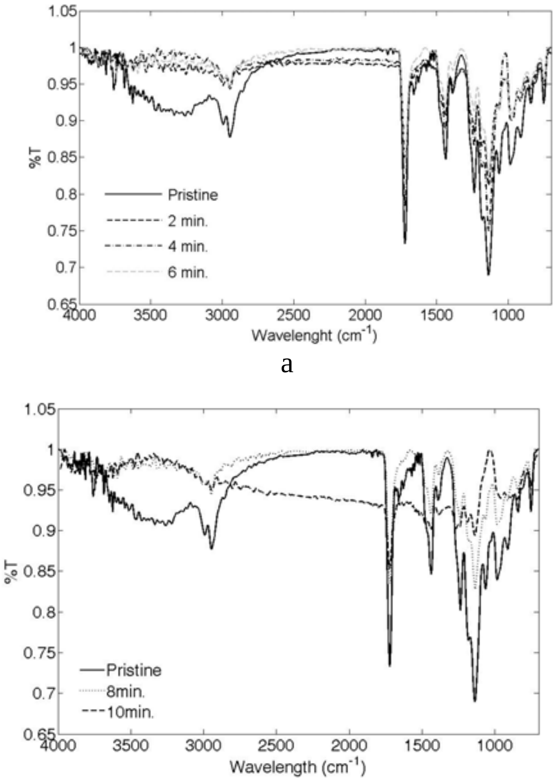

a

b

Fig. 3. ATR-FTIR spectrum for pristine sample beside treated samples for 2, 4 and 6 minutes (a) and 8 and 10 minutes (b) in nitrogen plasma.

In the case of N_2 plasma scenario is completely different. ATR- FTIR spectrum of the samples immersed in N_2 plasma is presented in Fig. 3. (a) and (b). As can be seen in Fig. 3 (a) after 2 minutes treatment in nitrogen plasma about 7% decrease occur in the transmission of PMMA sample in all the range of IR but in the range of 3200 to 3700 cm^{-1} the intensity of O-H broad peak decreases. ATR-FTIR spectrum of the 4, 6 and 8 minutes treatment samples are similar and very close to the pristine sample as is shown in Fig. 3 (a) and (b). All of them show a small increase in the transmission of IR radiation. And noticeable change is in the range of 2700 to 3700 cm^{-1}. The intensity of two peaks at 3000 and 3050 cm^{-1} belongs to C-H and H-C-H stretching group oscillations decreases and the O-H broad peak disappears completely. Fig. 3 (b) shows the spectrum of the sample which is treated in nitrogen plasma for 8 and 10 minutes. Absorption of IR radiation in these samples specially for the case of 10 minutes treated sample is decreased noticeably and the entire curve tends to be flat.

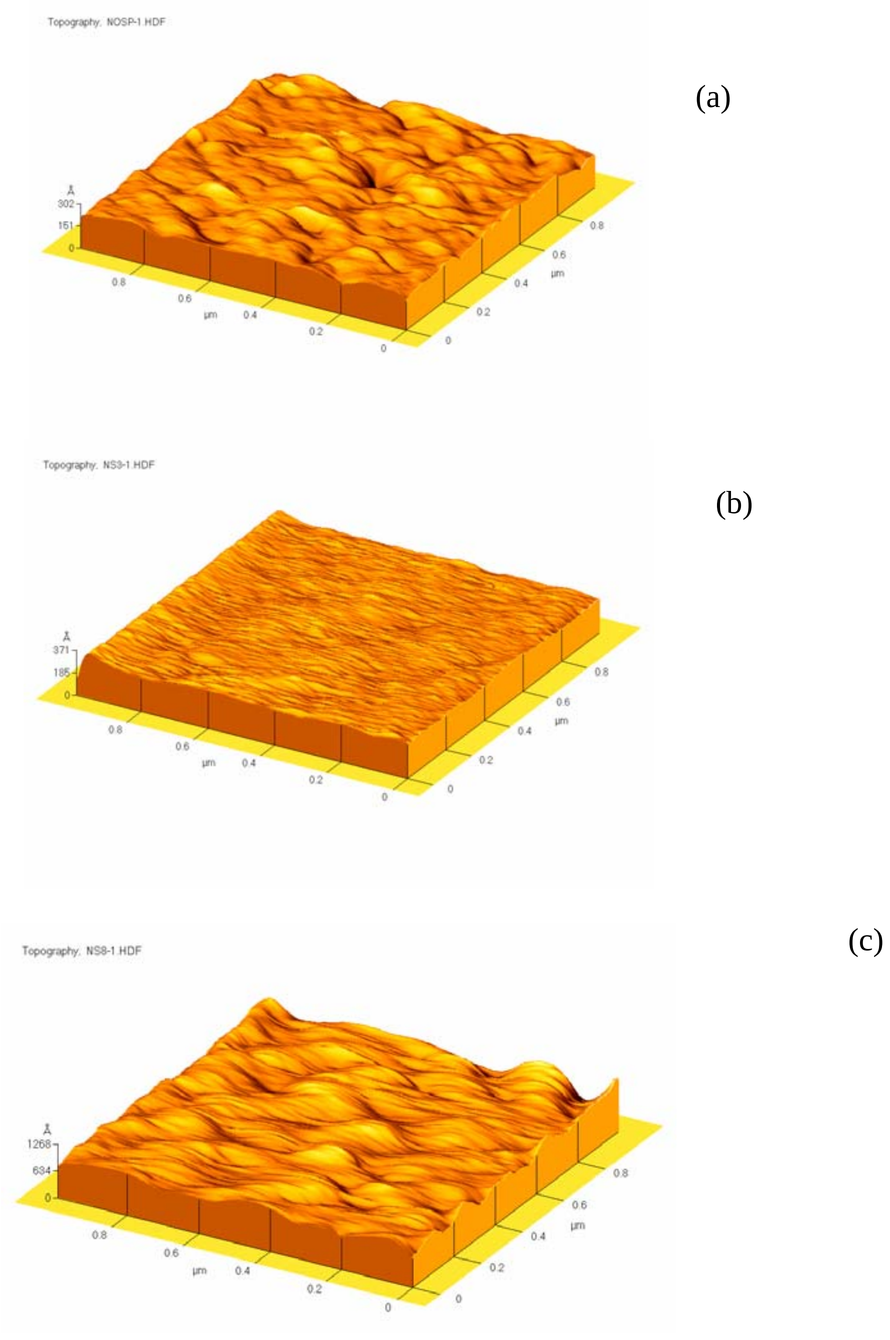

Fig. 4. AFM micrographs of a) pristine sample b) treated sample in oxygen plasma for 6 minutes c) treated sample in nitrogen plasma for 6 minutes.

Topologic changes of the surface of samples are investigated by AFM micrographs. They are shown in Fig. 4 just for 6 minutes treated samples in both oxygen and nitrogen plasmas as well as untreated sample. Compare to pristine sample, plasma treatment makes a relative uniformity on the surface of samples. Before treatment there is a nodule structure on the surface whose size decreases with treatment time. The RMS roughness of the surface versus treatment time for both kinds of samples treated in oxygen and nitrogen plasmas are plotted in Fig. 5. For the case of samples immersed in oxygen plasma RMS roughness varies between 20 to 40 Å randomly, while in the case of nitrogen treated samples RMS roughness increases with the time of treatment up to 6 minutes from 20 to 80 Å and after that again decrease to 20 Å in 10 minutes, which is probably due to defect enhanced surface diffusion. It is clear that nitrogen species in plasma hit the surface more strongly than oxygen so more effective on surface morphology and oxygen species in this range of energy is not influence on the surface topography. One expects that the roughness change has a direct impact on the surface properties, in particular on the wettability of the samples.

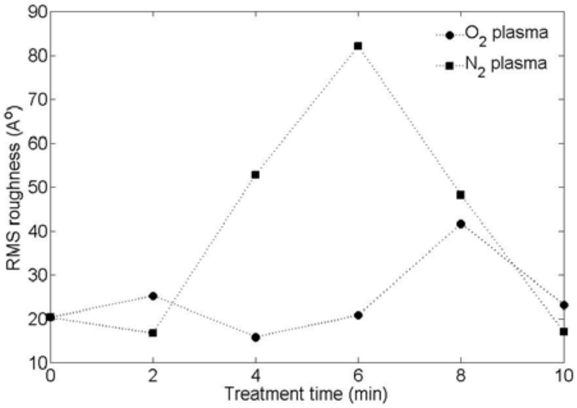

Fig. 5. RMS roughness of surface of samples versus treatment time.

Depending on the treatment duration, the weight loss per area unit corresponding to the degradation is shown in Fig. 6 which doesn't increase linearly with time of treatment. . As can be seen more than 60% of weight losing of about 3×10^{-4} gr/cm^2 is occurred in the first 2 minutes of treatment while after 2 minutes to 6 minutes this parameter is not changed and again in the last 2 minutes about 1×10^{-4} gr/cm^2 weight losing is occurred but not so rapidly compare to the first 2 minutes of treatment. According to AFM micrographs and RMS roughness this weight loss of samples confirm that plasma treatment degrade the surface irregularities to bear polar groups and removes the materials with less attachment energy to the surface.

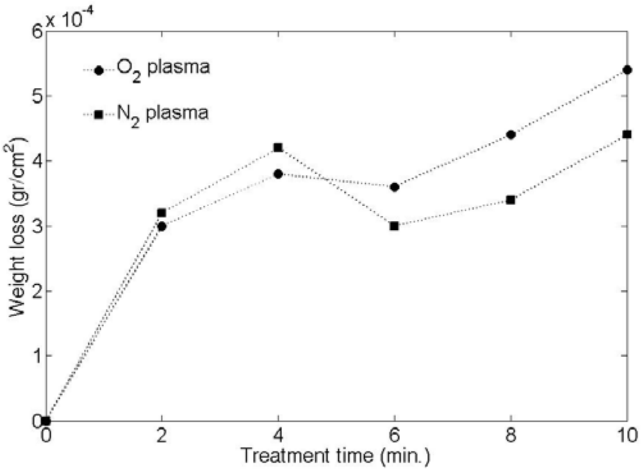

Fig. 6. Weight loss of samples per area unit versus treatment time.

3.2. Surface energy

Low energy RF plasmas are becoming widely accepted as a method of modifying polymer surface properties. In particular, the hydrophobicity of the surface can be tailored in this way. This is especially attractive for biocompatibility enhancements since cell adhesion is dependent on the surface energy of the polymer. Inert gas, oxygen, nitrogen and fluorine plasmas are all utilized for such purposes [13]. Surface energy is calculated by measuring the angle of contact of various wetting liquids. Surface energy has two components namely polar component (γ_s^p) and disperse component (γ_s^d). Both components contribute to total surface energy. The polar component is important to understand the hydrophilic surface modification, whereas the disperse component indicates the changes in hydrophobic modification or formation of cross-linked network [9]. The wetting ability is the ability of a liquid to adhere to a solid and spread over its surface. The classical model by Young suggests that:

$$\gamma_{SV} = \gamma_{LV} \cos\theta + \gamma_{SL} \tag{1}$$

where θ is the measured contact angle, γ_{sv} the surface tension of solid in contact with air, γ_{Lv} the surface tension of the liquid in contact with air, and γ_{sL} is the surface tension between the solid and the liquid. The work of adhesion W_a between the solid and liquid can be expressed in terms of the Dupre equation as follows:

$$W_a = \gamma_{SV}(1+\cos\theta) \tag{2}$$

The solid surface tension can be separated into the intermolecular attraction of polar interaction γ_s^p and dispersion interaction γ_s^d as:

$$\gamma_S = \gamma_S{}^d + \gamma_S{}^p \tag{3}$$

Therefore, the work of adhesion can be expressed as the sum of the different intermolecular forces at the interface.

$$W_a = 2(\gamma_{LV}{}^d \gamma_S{}^d)^{1/2} + 2(\gamma_{LV}{}^p \gamma_S{}^p)^{1/2} \tag{4}$$

then

$$\gamma_{LV}(1+\cos\theta) = 2(\gamma_{LV}{}^d \gamma_S{}^d)^{1/2} + 2(\gamma_{LV}{}^p \gamma_S{}^p)^{1/2} \tag{5}$$

For water: γ_{Lv} =72.8 mN/m, γ_{Lv}^d=21.8 mN/m, γ_{Lv}^p =51.0 mN/m.

And for diodomethane: γ_{Lv} =50.8 mN/m, γ_{Lv}^d =49.5 mN/m, γ_{Lv}^p =1.3 mN/m [10,14].

In order to understand the hydrophilic and hydrophobic modifications achieved on PMMA surface due to RF plasma treatment, γ_s^p and γ_s^d values of total surface energy are tabulated in table I. In table I also the water and diodomethane contact angle values of modified surfaces are presented. In Fig. 7 the total surface energy of N_2 and O_2 plasma modified PMMA sheets are presented. It can be seen that up to 8 minute of treatment time the value of surface energy for N_2 plasma modification is slightly higher than for O_2. For 10 minutes of plasma treatment, the O_2 treated sample shows higher value for surface energy in comparison with N_2. It can be seen that value of polar component of surface energy on the surface of nitrogen plasma treated sample increases gradually with treatment time up to 8 minutes treatment and after that decreases. In the case of samples treated with oxygen plasma the polar component of surface energy starts to decrease after 4 minutes treatment. In both cases the contribution of disperse part in the total energy of PMMA surfaces decreases and polar component becomes more effective due to plasma treatment which is resultant in the water contact angle variation. As mentioned above the surface energy is measured through Owens–Wendt and Wu methods. Results are very similar so in this part we only discuss on the data obtained by Owens–Wendt method.

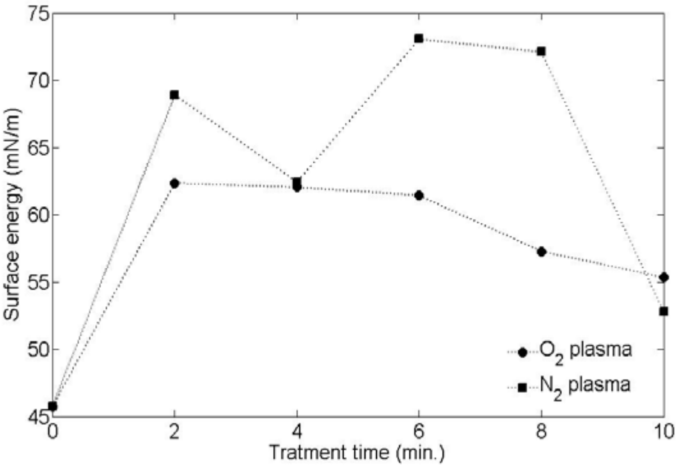

Fig. 7. Surface energy of treated samples versus treatment time with Owens-Wendt method.

Table 1. Values of disperse and polar parts of surface energy, and water and diodo-methan contact angles on the surface of oxygen and nitrogen treated samples.

	N_2 Plasma				O_2 plasma			
Treatment time (min.)	Water contact angle (^{o})	Diodo-methane contact angle (^{o})	γ_s^p (mN/m)	γ_s^d (mN/m)	Water contact angle (^{o})	Diodo-methane contact angle (^{o})	γ_s^p (mN/m)	γ_s^d (mN/m)
0	76.3	36.4	4.40	41.36	76.30	36.40	4.40	41.36
2	33.7	31.1	25.11	43.78	40.40	43.70	24.65	37.69
4	40.7	42.7	24.16	38.24	40.80	44.10	24.52	37.52
6	21.2	37.2	32.07	41.00	43.60	40.10	21.85	39.58
8	23.6	37.5	31.26	40.83	50.10	41.40	18.38	38.91
10	55.4	46.1	16.34	36.43	52.70	42.90	17.22	38.12

The water contact angle of treated samples is plotted in Fig. 8. The hydrophobicity of surface is strongly affected not only by the chemical composition but also by the roughness of surface [15]. As can be seen here for both mentioned treatment specially in the case of oxygen plasma treated samples roughness is not varied effectively so changes in the magnitude of water contact angle is mainly due to changes in surface molecular structure. ATR-FTIR results in Figs. 2 and 3 confirm that specially for the case of samples treated in nitrogen plasma the hydroxyl/ hydro peroxide (absorbing at 3000 to 3600 cm-1) are mainly responsible for the increase of sample wettability. Comparison between Figs. 7 and 8 shows that rate of variation of water contact angle on the surface of samples is exactly the inverse rate of variation of surface energy. The contact angle of nitrogen plasma treated sample after 6 minutes treating reaches to 21.2 degree from 76.3 degree of pristine sample shows that PMMA hydrophilic property is so sensitive to RF nitrogen plasma treatment however all treated samples are more hydrophilic than the pristine one.

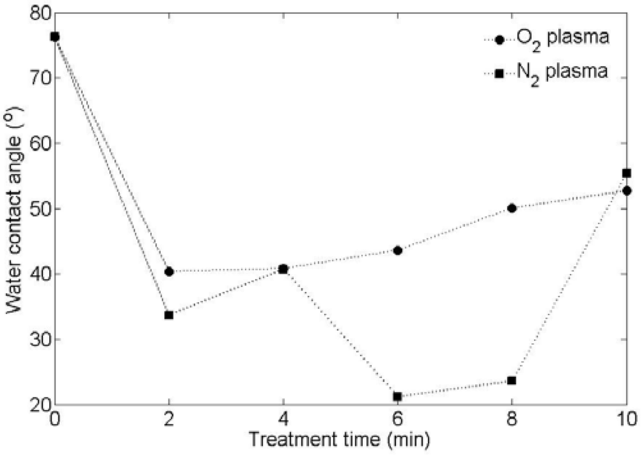

Fig. 8. Water contact angle on the surface of treated samples versus treatment time.

3.3. Determination of optical constants:

The optical properties of the samples can be characterized by the complex refractive index. The complex refractive index is expressed as

$$\hat{n} = n(\omega) + ik(\omega) \tag{6}$$

where n is the real part and k is the imaginary part of it. n can be obtained from the following equation [16]

$$n = (\frac{1+R}{1-R}) + \sqrt{\frac{4R}{(1-R)^2} - k^2} \tag{7}$$

where $k=\alpha\lambda/4\pi$.

Transmission and reflection spectrums of the samples can be converted to the absorption coefficient using the following relation

$$\alpha = \frac{1}{d}\ln\left[\frac{(1-R)^2}{2T} + \sqrt{\frac{(1-R)^4}{4T^2} + R^2}\right] \tag{8}$$

where α is the absorption coefficient and d is the thickness of sample. The values of n for both kinds of samples are shown in Fig. 9 (a) for oxygen plasma treated samples and (b) for nitrogen plasma treated samples. In the visible range of electromagnetic spectrum, the refractive index n of both kinds of samples is below 1.2. This value of the refractive index of samples is much lower than that of hard amorphous hydrogenated carbon samples, which in the visible range varies from 1.9 to 2.3 [15]. It is observed that for pristine PMMA sheet there is anomalous dispersion at $\lambda <$ 350 nm as well as normal dispersion at $\lambda >$ 350 nm. This is a transition behavior between the multi oscillator to single oscillator model developed by Wemple and Didomenico [17]. On the other hand, for treated samples there is not any anomalous dispersion in all measured region of wavelengths.

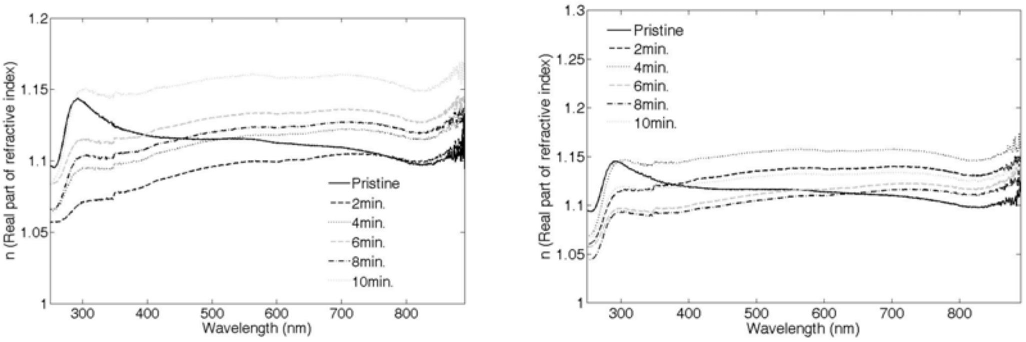

a b

Fig. 9. Real part of refractive index of different wavelength for treated samples with oxygen plasma (a) and with nitrogen plasma (b).

In Fig. 10 the imaginary part of refractive index k for oxygen (a) and nitrogen (b) plasma treated samples is shown. In the case of treating with oxygen plasma imaginary part of refractive index increases with treatment time specially in NIR range but nitrogen plasma treatment doesn't affect this parameter noticeably.

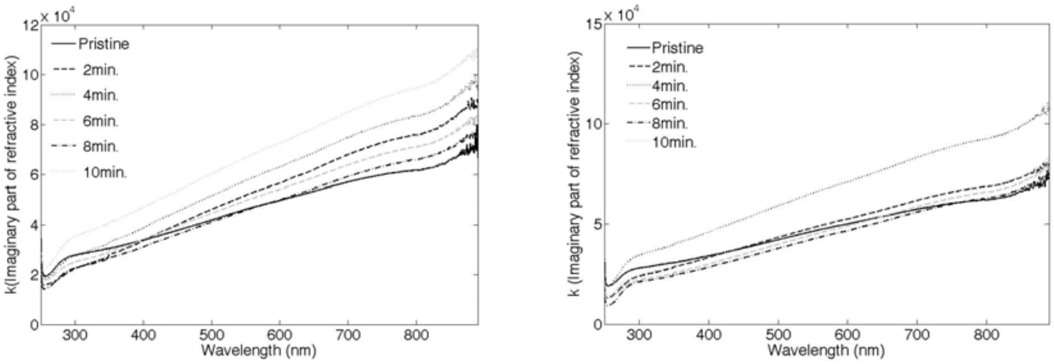

a b

Fig. 10. Imaginary part of refractive index for different wavelength of treated samples with oxygen plasma (a) and with nitrogen plasma (b).

The complex dielectric constant is described as

$$\hat{K} = K_r + iK_I \tag{9}$$

where K_r is the real part and K_I is the imaginary part of the dielectric constant. The imaginary and real parts of dielectric constant are expressed as [18]

$$K_r = n^2 - k^2 \tag{10}$$

and

$$K_I = 2nk \tag{11}$$

The real part of the dielectric constant relates to the dispersion, while the imaginary part provides a measure of the dissipative rate of the wave in the medium.

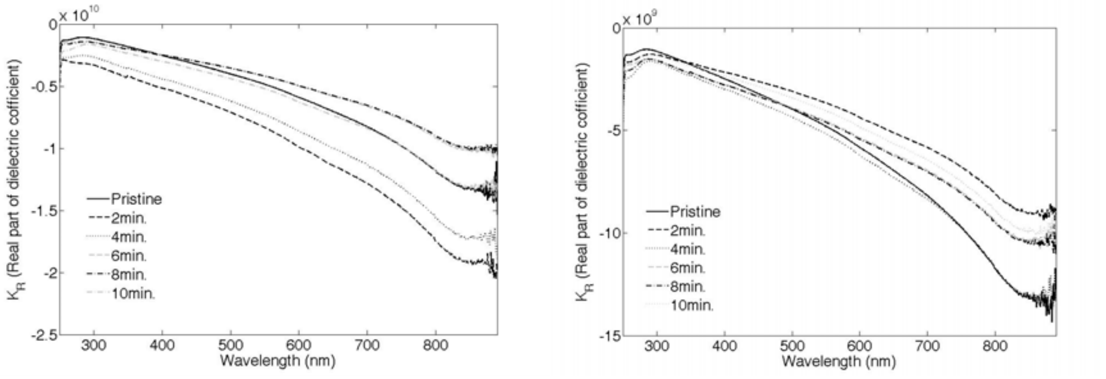

a b

Fig. 11. Real part of dielectric constant versus wavelength for treated samples with oxygen plasma (a) and with nitrogen plasma (b).

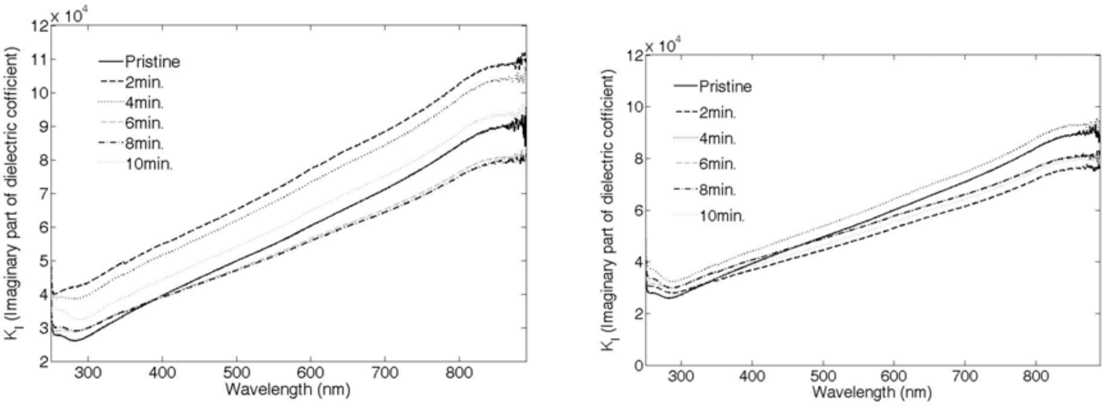

a b

Fig. 12. Imaginary part of dielectric constant versus wavelength for treated samples with oxygen plasma (a) and with nitrogen plasma (b).

Figs. 11 (a) and (b) and 12 (a) and (b) show the real and imaginary parts dependence on wavelength respectively. As can be seen in figures for the case of nitrogen treated samples the real part of dielectric constant is increased with increasing the treatment time in the range of NIR but by oxygen treatment this increase is occurred for the imaginary part of dielectric constant which suggest that dielectric loss increases after treatment. The real part of dielectric constant decreases for the samples treated by oxygen plasma less that 6 minutes and increases for the samples which are treated for more than 6 minutes which occurs inversely for the real part.

3. 4. Determination of optical band gap:

The optical band gap is the value of optical energy gap between the valance band and the conduction band. The optical band gap of the samples is determined from the absorption spectra near the absorption edges. The photon absorption in many amorphous materials is found to obey the Tauce relation [4,11], which is of the form

$$\alpha h\nu = B(h\nu - E_g)^n \tag{12}$$

where α is the absorption coefficient, $h\nu$ is the photon energy, factor *B* depends on the transition probability and can be assumed to be constant within the optical frequency range [19], and the index *n* is related to the distribution of the density of states. The index *n* has discrete values like

1/2, 3/2, 2 or more depending on whether the transition is direct or indirect and allowed or forbidden, respectively. In the direct and allowed cases, the index n=1/2 whereas for the direct but forbidden cases it is 3/2. But for the indirect and allowed cases n=2 and for the forbidden cases it is 3 or more. The value of n for samples is estimated from the slop of the log(α) vs log($h\nu$) plots by taking a linear fit is found to be 2 [19,20]. To calculate E_g, the usual method is plotting $(h\alpha\nu)^{1/n}$ against $h\nu$. The values of the band gap energy of pristine and treated samples are tabulated in Table II. As can be seen this magnitude is not changed in the treatment process due to low power of the applied plasma.

Table 2. Values of the band gap of the pristine and treated samples.

	E_g (eV)	
Treatment time(min.)	O_2 plasma	N_2 plasma
0	4.920	4.920
2	4.910	4.930
4	4.920	4.910
6	4.930	4.920
8	4.915	4.910
10	4.920	4.920

4. Conclusion

In this work the surface of PMMA sheets are treated by low power RF nitrogen and oxygen plasmas. Nitrogen plasma is more effective on the topology of the surface while the molecular structure of the surfaces is much more affected by oxygen plasma treatment. Results confirm that such low power RF plasma is sufficient to change the surface energy and improve the wettability of PMMA surface. In this regime the weight of PMMA doesn’t change noticeably. By applying RF plasmas in this range of power optical constants and properties as well as band gap energy of PMMA do not change effectively.

Acknowledgement

Authors like to acknowledge professor Jaleh in Physics Department of Hamedan University, Hamedan, Iran for providing us the PMMA sheets and because of his useful comments.

References

[1] N. L. Singh, A. Qureshi, F. Singh, D. K. Avasthi , Mater. Sci. Eng., B **137**, 85 (2007)
[2] R. K. Y. Fu, I. T. L. Cheung, Y. F. Mei, C. H. Shek, G. G. Siu, P. K. Chu, W. M. Yang, Y. X. Leng, Y. X. Huang, X. B. Tian, S. Q. Yang , Nucl. Instrum. Methods Phys. Res., Sect. B **237**, 417 (2005)
[3] H. Kaczmarek, H. Chaberska, Appl. Surf. Sci. **252**, 8185 (2006)
[4] F. Yakuphanoglu, G. Barim, I. Erol , Physica B **391**, 136 (2007)
[5] W. S. Kim, Y. C. Jeong, J. K. Park, C. W. Shin, N. Kim, Opt. Mater. **29**, 1736 (2007)
[6] M. Ozdemir, C. U. Yurteri, H. Sadikoglu , Crit. Rev. Food Sci. Nutr. **39**, 457 (1999)
[7] M. Yedji, G. G. Ross , Nucl. Instrum. Methods Phys. Res., Sect. B **256**, 396 (2006)

[8] W. C. A. Bento, R. Y. Honda, M. E. Kayama, W. H. Schreiner, N. C. Cruz, and E. C. Rangel, Plasmas Polym. **8**, 1 (2003)
[9] N. V. Bhat, D. J. Upadhyay, Plasmas Polym. **8**, 99 (2003)
[10] W. Zhang, P. K. Chu, J. Ji, Y. Zhang, Z. Jiang , Appl. Surf. Sci. **252**, 7884 (2006)
[11] S. Saravanan, M. R. Anantharaman, S. Venkatachalam, D. K. Avasthi, Vacuum **82**, 56 (2007)
[12] L. E. Nita, A. Ioanid, C. M. Popescu, I. Neamtu, G. E. Ioanid, A. P. Chiriac, Rom. Journ. Phys. **50**, 755 (2005)
[13] C. M. Chan, T. M. Ko, H. Hiroaka, Surf. Sci. Rep. **24**, 1 (1996)
[14] M. Aouinti, P. Bertrand, and F. P. Epaillard, Plasmas Polym. **8**, 225 (2003)
[15] K. Kutasi, N. Bibinov, A. Von Keudell, K. Wiesemann, J. Opto-electron. Adv. Mater. **7**, 2549 (2005)
[16] D. Dragoman, M. Dragoman, *Optical characterization of solids*, 1st edn. (Springer, Berlin, 2002)
[17] S. H. Wemple, M. DiDomenico, Phys. Rev. B **3**, 1338 (1971)
[18] J. R. Reitz, F. J. Milford, R. W. Christy, *Foundations of electromagnetic theory*, 1st edn. (Addison Wesley, 1992)
[19] H. M. Zidan, M. Abu-Elnader, Physica B **355**, 308 (2005)
[20] U. S. Sajeev, C. J. Mathai, S. Saravanan, R. R. Ashokan, S. Venkatachalam, M. R. Anantharaman, Bull. Mater. Sci. **29**, 159 (2006)